# Supporting Information

## Damo et al. 10.1073/pnas.1220341110

### SI Materials and Methods

**Strains.** The bacterial strains used in this study include *Staphylococcus aureus* strain Newman, *Staphylococcus epidermidis* strain ATCC 12228, *Staphylococcus lugdunensis* strain N920143, *Enterococcus faecalis* strain OGIRF, *Acinetobacter baumannii* strain 17978, *Pseudomonas aeruginosa* strain PA01, *Escherichia coli* strain DH5α, and *Shigella flexneri* SC560 (an M90T derivative with a ΔicsA::ΩSp$^r$ mutation). All stocks were maintained at −80 °C, and bacteria were routinely grown in tryptic soy broth (TSB) or brain heart infusion broth (BHI).

**Calprotectin Antimicrobial Activity Assays.** The $IC_{50}$ experiments were performed as previously described (1). Briefly, bacteria were grown overnight at 37 °C in 5 mL TSB in a 15-mL conical tube on a roller drum. The next morning the bacteria were back-diluted 1/50 into 5 mL fresh TSB in a 15-mL conical tube and grown for 1 h at 37 °C on a roller drum. Following this incubation, exponential-phase bacteria were diluted 1/100 into 96-well round-bottom plates that contained 38% (vol/vol) TSB and 62% (vol/vol) calprotectin buffer (100 mM NaCl, 3 mM $CaCl_2$ 10 mM β-mercaptoethanol, 20 mM Tris, pH 7.5) and various concentrations of WT or mutant calprotectin (CP). Bacteria were grown at 37 °C with shaking, and optical density ($OD_{600}$) was used to monitor growth. For $IC_{50}$ experiments, growth at 7 h was examined ($n = 17$ for WT CP, 13 for ΔS1, 12 for ΔS2, and 5 for the C→S mutant). For experiments using stationary-phase bacteria, the 5-mL subculture was omitted, and the overnight cultures were directly inoculated (1/100) into the assay media. For experiments examining the antimicrobial activity of CP and mutant derivatives toward a range of species, overnight cultures were performed in BHI and were directly inoculated (1/100) into 38% (vol/vol) BHI and 62% (vol/vol) CP buffer with only 5 mM beta-mercaptoethanol.

**Oxidative Stress Assays.** Experiments intended to test the ability of CP mutants to increase staphylococcal sensitivity to superoxide stress, elevate intracellular superoxide, and inhibit *S. aureus* superoxide dismutase (SOD) activity were performed as previously described and are therefore only briefly described below (1). For all three assays, bacteria were grown overnight at 37 °C in 5 mL TSB in a 15-mL conical tube on a roller drum. The next morning the overnight culture was diluted 1/100 into 96-well round-bottom plates containing growth media. The media consisted of 38% BHI with 0.5% glucose and 62% (vol/vol) calprotectin buffer and was supplemented with various concentrations of WT CP, the ΔS1 mutant, the ΔS2 mutant, $MnCl_2$, and the superoxide-generating compound paraquat. The bacteria were then grown at 37 °C with shaking. For experiments designed to test the ability of the CP mutants to increase the sensitivity of *S. aureus* to superoxide stress, growth was assessed by measuring $OD_{600}$. For intracellular superoxide accumulation assays, after 7 h of growth bacteria were incubated with dihydroethidium for 35 min, washed with PBS, and analyzed by FACS for ethidium bromide fluorescence. To assess SOD activity, bacteria were grown to exponential phase in the presence of protein and 1 mM paraquat to increase SOD activity and then harvested, washed, and lysed via bead beating. Total SOD activity was determined via water-soluble tetrazolium salt assay (Sigma-Aldrich), and protein concentration was quantified via bicinchoninic acid assay (Pierce Thermo-Fisher).

**Elemental Analysis.** Metal concentrations in TSB and BHI were assessed by high-resolution inductively coupled plasma mass spectrometry (HR-ICPMS). Quantitative analysis of elements of interest (Mg, P, Ca, Mn, Fe, Co, Cu, and Zn) was performed using a Thermo Element 2 HR-ICPMS methods (Thermo Fisher Scientific) equipped with an ESI auto sampler (Elemental Scientific), a Perfluoroalkoxy microflow nebulizer (Elemental Scientific), a double-channel spray chamber (at room temperature), a magnetic sector followed by an electric sector, and a second electron multiplier (SEM). The samples were first taken up by self-aspiration via a 0.50-mm internal diameter sample probe and transferred to the nebulizer and spray chamber. The fine sample aerosol formed in the spray chamber was then transported by argon gas to hot plasma for vaporization, atomization, and ionization. All analyte ions were filtered and separated by magnetic sector and electric sector for the selected elemental isotopes that were detected by SEM. The operation parameters of HR-ICPMS are listed in Table S3.

**CP Mutant Construction.** To create the calprotectin site I and site II mutants, expression vectors containing S100A8 and S100A9 were sequentially mutated by site-directed mutagenesis. The primers used to create each mutation were as follows:

S100A8 H17N (fwd-CTCTATCATCGACGTCTACAACAAGTACTCCCTGATAAA, rev-TTTATCAGGGAGTACTTGTTGTAGACGTCGATGATAGAG),

S100A8 H27N (fwd-CCCTGATAAAGGGGAATTTCAATGCCGTCTACAGGG, rev- CCCTGTAGACGGCATTGAAATTCCCCTTTATCAGGG),

S100A8 H87N (fwd-GCAGCCCACAAAAAAAGCAATGAAGAAAGCCACAAAG, rev-CTTTGTGGCTTTCTTCATTGCTTTTTTTGTGGGCTGC),

S100A8 H81N, H87N (fwd-GGCGTGGCAGCCAACAAAAAAAGCAATGAAGAAAGCCAC, rev-GTGGCTTTCTTCATTGCTTTTTTTGTTGGCTGCCACGCC),

S100A9 H20N (fwd-ACCATCATCAACACCTTCAACCAATACTCTGTGAAGC, rev- GCTTCACAGAGTATTGGTTGAAGGTGTTGATGATGGT),

S100A9 D30S (fwd-AGCTGGGGCACCCATCCACCCTGAACCAGG, rev-CCTGGTTCAGGGTGGATGGGTGCCCCAGCT),

S100A9 H95N (fwd-CCCACGAGAAGATGAACGAGGGTGACGAG, rev-CTCGTCACCCTCGTTCATCTTCTCGTGGG),

S100A9 H91N, H95N (fwd-CTAACCTGGGCCTCCAACGAGAAGATGAACG, rev-CGTTCATCTTCTCGTTGGAGGCCCAGGTTAG),

S100A9 H103N, H104N, H105N (fwd-GACGAGGGCCCTGGCAACAACAATAAGCCAGGCCTCGG, rev-CCGAGGCCTGGCTTATTGTTGTTGCCAGGGCCCTCGTC).

For multistep mutations, if the second primer set overlapped a previously introduced alteration, this change was incorporated into the oligo. All constructs were sequenced to ensure that only the targeted nucleotides were mutated.

1. Kehl-Fie TE, et al. (2011) Nutrient metal sequestration by calprotectin inhibits bacterial superoxide defense, enhancing neutrophil killing of *Staphylococcus aureus*. *Cell Host Microbe* 10(2):158–164.

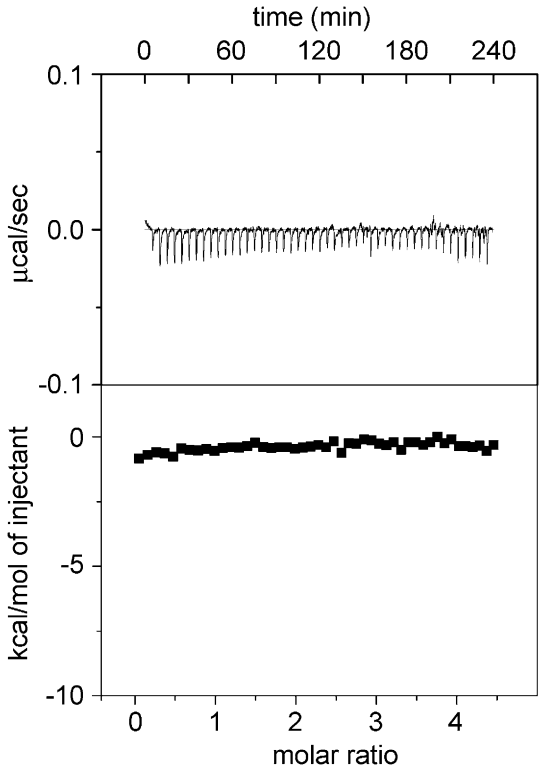


**Fig. S1.** CP does not bind iron. Isothermal titration calorimetry and binding isotherm from integrated heat for CP are shown for the addition of Fe, revealing no binding of this ion.

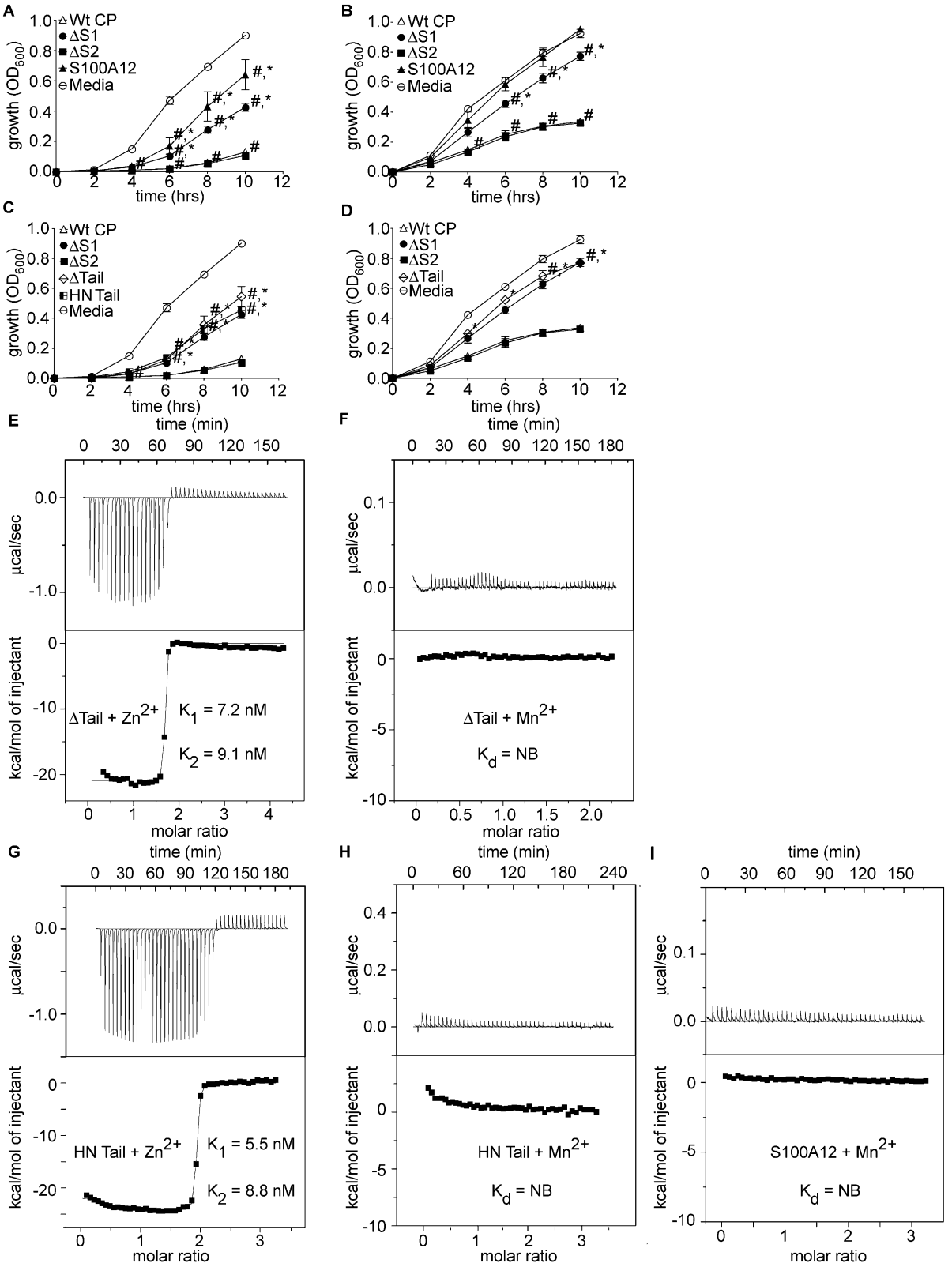


**Fig. S2.** Mn sequestration is necessary for inhibition of *S. aureus* growth. WT CP, ΔS1, ΔS2, ΔTail, HN Tail, and S100A12 were characterized for antimicrobial activity and metal binding. (*A–D*) To evaluate the contributions of Mn and Zn binding to inhibition of staphylococcal growth, *S. aureus* was grown in media alone or with 960 μg/mL of WT CP, the ΔS1 binding-site mutant, the ΔS2 binding-site mutant, (*C* and *D*) ΔTail mutant, (*A* and *B*) S100A12, or (*C*) HN Tail. Cultures were started with (*A* and *C*) exponential or (*B* and *D*) stationary-phase bacteria, and growth was assessed by optical density ($OD_{600}$); $n = 3–6$. The symbols for WT CP and ΔS2 frequently overlap. Statistical significance was determined via two-way ANOVA with Bonferroni posttest $^{\#}P < 0.05$ relative to media; $^{*}P < 0.05$ relative to WT CP. Error bars: SEM. (*E* and *F*) Isothermal titration calorimetry (ITC) titrations and binding isotherms from integrated heat for

Legend continued on following page

the ΔTail mutant shown for addition of (*E*) Zn [$K_d = 9.1 \pm 1.1$ (SD) and $7.2 \pm 1.2$ (SD) nM] and (*F*) Mn (no binding). (*G* and *H*) ITC titrations and binding isotherms from integrated heat for the HN Tail mutant shown for addition of (*E*) Zn [$K_d = 5.5 \pm 1.4$ (SD) and $8.8 \pm 1.3$ (SD) nM] and (*H*) Mn (no binding). (*I*) ITC titration and binding isotherm from integrated heat for S100A12 are shown for addition of Mn, revealing no binding of this ion.

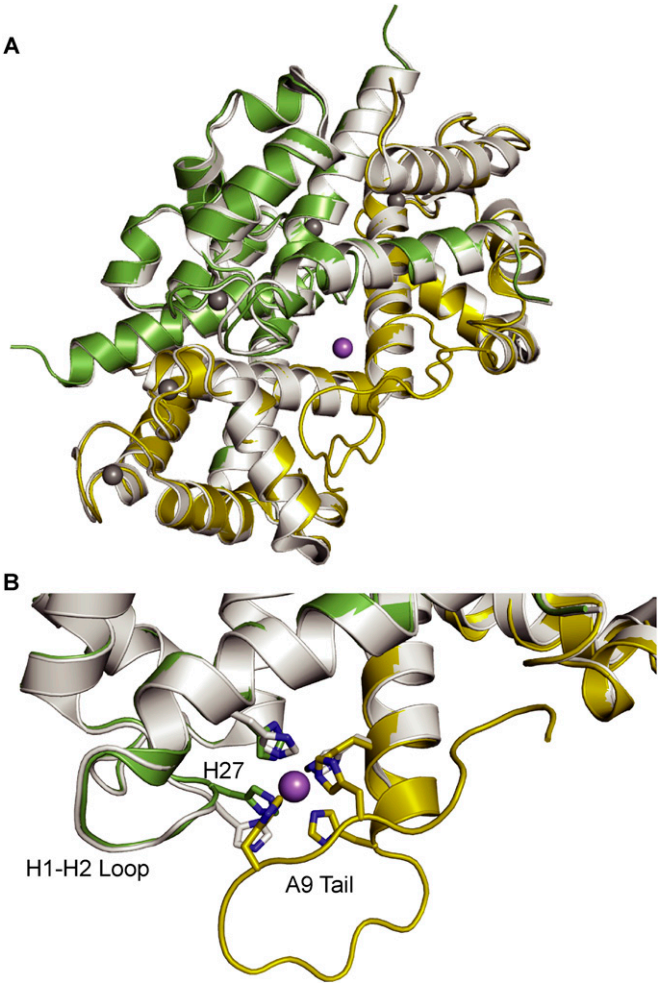


**Fig. S3.** Conformational changes of CP upon Mn binding. The quaternary structure of CP is composed of a heterotetramer. Ca ions are shown as gray spheres; Mn is shown in purple. (*A*) Superposition of $Ca^{2+}$-bound (gray) and Ca/Mn-bound (S100A8 in green, S100A9 in yellow) CP reveals no large-scale conformational changes induced by the binding of Mn. (*B*) A minor rearrangement of the loop connecting helices 1 and 2 optimally positions H27 of S100A8 for Mn binding. Structural ordering of the S100A9 tail is essential for Mn binding.

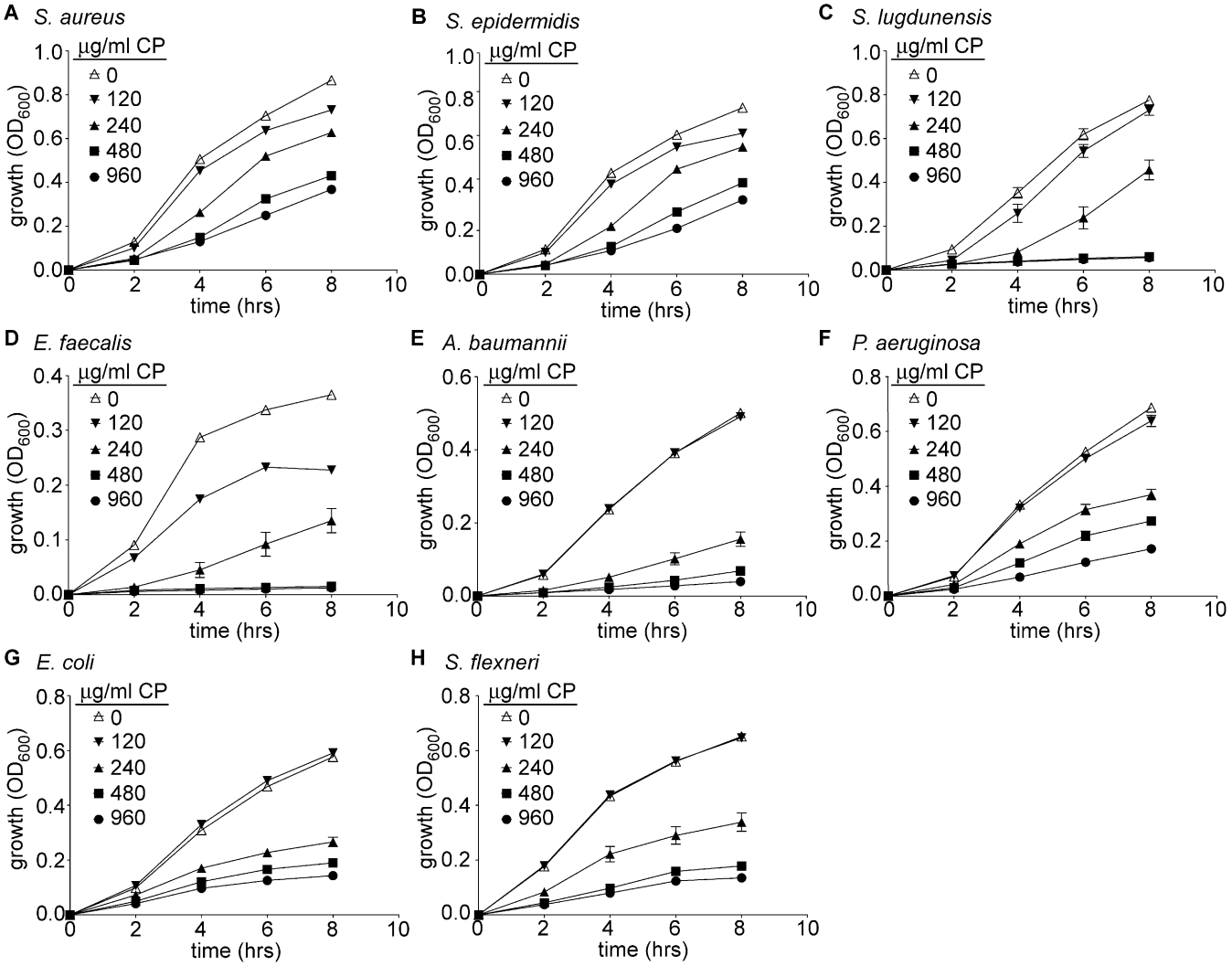


**Fig. S4.** CP is broadly antimicrobial. (*A*–*H*) To evaluate the antimicrobial activity of CP toward a range of pathogens, (*A*) *S. aureus*, (*B*) *S. epidermidis*, (*C*) *S. lugdunensis*, (*D*) *E. faecalis*, (*E*) *A. baumannii*, (*F*) *P. aeruginosa*, (*G*) *E. coli*, or (*H*) *S. flexneri* were grown in media alone or in the presence of increasing concentrations of CP. Growth was assessed by measuring optical density ($OD_{600}$). $n = 3$–4. Error bars represent SEM.

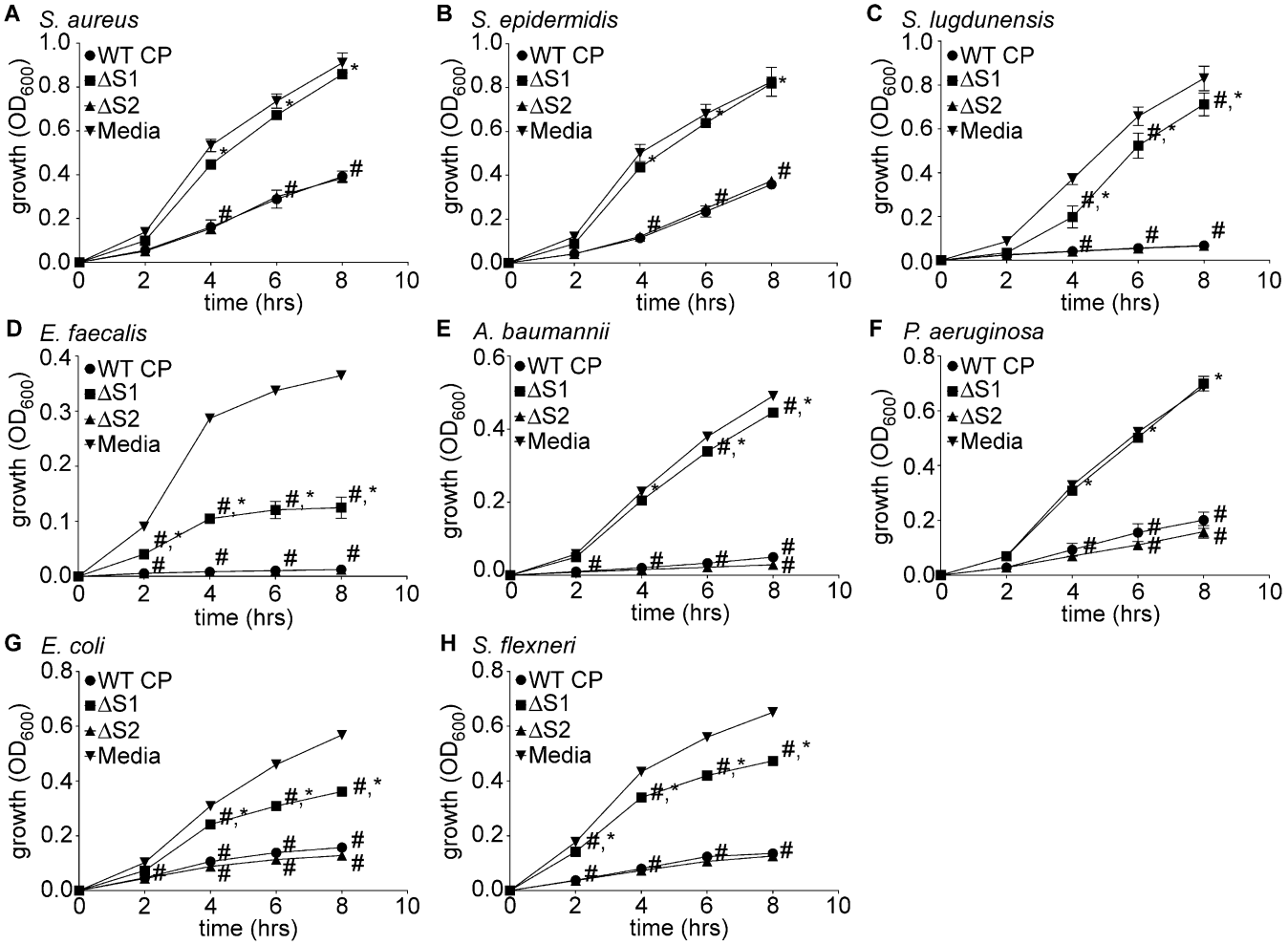


**Fig. S5.** Broad-spectrum antimicrobial activity of CP is dependent on Mn sequestration. (*A–H*) To evaluate the contribution of Mn binding to the antimicrobial activity of CP, (*A*) *S. aureus*, (*B*) *S. epidermidis*, (*C*) *S. lugdunensis*, (*D*) *E. faecalis*, (*E*) *A. baumannii*, (*F*) *P. aeruginosa*, (*G*) *E. coli*, or (*H*) *S. flexneri* were grown in media alone or in the presence of 960 μg/mL WT CP, the ΔS1 mutant, or the ΔS2 mutant. Growth was assessed by measuring optical density ($OD_{600}$). The symbols of WT CP and ΔS2 frequently overlap. Statistical significance was determined via two-way ANOVA with Bonferroni posttest $^{\#}P < 0.05$ relative to media; $^{*}P < 0.01$ relative to WT CP. $n = 3$–4. Error bars represent SEM.

**Table S1. Elemental analysis of growth media**

| Element | BHI | BHI CP media* | TSB | TSB CP media* |
|---|---|---|---|---|
| Magnesium, μM | 61.3 ± 48.9 | 23.3 | 122.4 ± 11.5 | 46.5 |
| Phosphorous, μM | 5,635.8 ± 126.4 | 2,141.6 | 5,048.0 ± 51.94 | 1,918.2 |
| Calcium, μM | 39.2 ± 9.0 | 1.9 (mM) | 43.0 ± 4.9 | 1.9 (mM) |
| Iron, μM | 2.0 ± 0.8 | 0.8 | 1.9 ± 0.1 | 0.7 |
| Zinc, μM | 2.4 ± 1.47 | 0.9 | 1.5 ± 0.2 | 0.6 |
| Manganese, nM | 74.8 ± 27.8 | 28.4 | 106.7 ± 11.7 | 40.6 |
| Copper, nM | 39.1 ± 25.6 | 14.8 | 23.4 ± 3.3 | 8.9 |
| Cobalt, nM | 50.2 ± 39.8 | 19.1 | 28.5 ± 1.6 | 10.8 |

*Concentration calculated for media that contains 38% (vol/vol) TSB or BHI and 62% (vol/vol) calprotectin buffer. $n = 3$ independent media preparations. ±SD

**Table S2. Data collection and refinement statistics**

| | | |
|---|---|---|
| Data collection | | |
| Wavelength | 0.978 Å | 1.887 Å |
| Space group | $P2_12_12$ | |
| Cell dimensions | | |
| *a*, *b*, *c*; Å | 82.03, 217.00, 53.02 | |
| α, β, γ; ° | 90.00, 90.00, 90.00 | |
| Resolution, Å | 50–1.6(1.7–1.6) | 50–2.0 (2.1–2.0) |
| $R_{meas}$ | 7.8 (80.4) | 7.98 (62.1) |
| $I/\sigma I$ | 16.7 (2.05) | 13.6 (2.2) |
| Completeness, % | 98.6 (92.2) | 98.2 (89.9) |
| Redundancy | 6.7 (4.7) | 4.4 (3.2) |
| Refinement | | |
| Resolution, Å | 50–1.6 | |
| No. of reflections | 117,923 | |
| $R_{work}/R_{free}$ | 17.7/20.2 | |
| No. of atoms | | |
| Protein | 6735 | |
| Ligand/ion | 19 | |
| Water | 488 | |
| *B*-factors | | |
| Protein | 23.44 | |
| Ligand/ion | 18.96 | |
| Water | 29.77 | |
| rmsd | | |
| Bond lengths, Å | 0.016 | |
| Bond angles, ° | 1.68 | |

Values in parentheses are for highest-resolution shell.

**Table S3. HR-ICPMS parameters**

| | |
|---|---|
| Radio frequency power | 1,250 W |
| Cool gas | 16.00 L·min$^{-1}$ |
| Auxiliary gas | 0.8 L·min$^{-1}$ |
| Sample gas | 0.97 L·min$^{-1}$ |
| Resolution mode | Medium resolution (4,300) |
| Isotopes measured | $^{25}$Mg, $^{31}$P, $^{42}$Ca, $^{55}$Mn, $^{56}$Fe, $^{59}$Co, $^{63}$Cu, $^{66}$Zn |
| Runs | 10 |
| Passes | 1 |
| Samples per peak | 20 |
| Sample time | 0.01 s |

**Table S4. Summary of ITC measurements**

| Sample | $K_d$ S1, nM | $K_d$ S2, nM | ΔH, kcal/mol | *n* | *c* |
|---|---|---|---|---|---|
| CP ΔS1 + $Zn^{2+}$ | n.b. | 8.2 ± 1.5 | −22.1 ± 1.5 | 1.7 ± 0.2 | 2,439 |
| CP ΔS1 + $Mn^{2+}$ | n.b. | n.b. | — | — | — |
| CP ΔS2 + $Zn^{2+}$ | 3.4 ± 1.2 | n.b. | −20.3 ± 1.2 | 0.9 ± 0.1 | 2,741 |
| CP ΔS2 + $Mn^{2+}$ | 5.8 ± 1.6 | n.b. | −26.4 ± 2.1 | 0.8 ± 0.2 | 2,229 |
| CP ΔTail + $Zn^{2+}$ | 7.2 ± 1.2* | 9.1 ± 1.1* | −20.0 ± 0.9 | 1.5 ± 0.3 | 2,456 |
| CP ΔTail + $Mn^{2+}$ | n.b. | n.b. | — | — | — |
| CP HN Tail + $Zn^{2+}$ | 5.5 ± 1.4* | 8.8 ± 1.3* | −23.2 ± 1.8 | 1.9 ± 0.3 | 2,797 |
| CP HN Tail + $Mn^{2+}$ | n.b. | n.b. | — | — | — |
| CP + $Fe^{3+}$ | n.b. | n.b. | — | — | — |
| S100A12 + $Mn^{2+}$ | n.b. | n.b. | — | — | — |

*n*, number of binding sites; $c = n \cdot K_d \cdot$ (protein), a unitless parameter chosen to be between 1 and 3,000. n.b., no binding.

*Data were fit to a two-site binding model; $K_d$ values for S1 and S2 were assigned on the basis of the results of the measurements made for the ΔS1 and ΔS2 mutants ±SD.